University of Massachusetts Amherst
ScholarWorks@UMass Amherst

Astronomy Department Faculty Publication Series | Astronomy

2005

Black hole X-ray binaries LMC X–1 and X–3: observations confront spectral models

Y Yao

QD Wang
University of Massachusetts - Amherst

SN Zhang

Follow this and additional works at: https://scholarworks.umass.edu/astro_faculty_pubs

 Part of the Astrophysics and Astronomy Commons

Recommended Citation
Yao, Y; Wang, QD; and Zhang, SN, "Black hole X-ray binaries LMC X–1 and X–3: observations confront spectral models" (2005). *MonMonthly Notices of the Royal Astronomical Society*. 1050.
10.1111/j.1365-2966.2005.09294.x

This Article is brought to you for free and open access by the Astronomy at ScholarWorks@UMass Amherst. It has been accepted for inclusion in Astronomy Department Faculty Publication Series by an authorized administrator of ScholarWorks@UMass Amherst. For more information, please contact scholarworks@library.umass.edu.

Mon. Not. R. Astron. Soc. **000**, 1–?? (2002) Printed 5 February 2008 (MN LATEX style file v2.2)

Black Hole X-ray Binary LMC X–1 and LMC X–3: Observations Confront Spectral Models

Yangsen Yao[1⋆], Q. Daniel Wang[1], and Shuang Nan Zhang[2]
[1] *Department of Astronomy, University of Massachusetts, Amherst, MA 01003;*
[2] *Department of Physics, University of Alabama, Huntsville, AL 35899*

arXiv:astro-ph/0508086v1 2 Aug 2005

Accepted 2005 xxxx xx. Received 2005 January xx; in original form 2005 xxxx xx

ABSTRACT
We present a comprehensive spectral analysis of black hole X-ray binaries, LMC X–1 and LMC X–3, based on *BeppoSAX* observations. We test both the multi-color disk plus power law (MCD+PL) model and a newly-developed Monte-Carlo simulation-based model for a Comptonized MCD (CMCD) with either a spherical or a slab-like corona, by comparing the inferred parameters with independent direct measurements. While all models give an adequate description of the spectra, we find a significant discrepancy between the MCD+PL inferred X-ray-absorbing gas column density and the absorption-edge measurement based on dispersed X-ray spectra. The MCD+PL fits to the LMC X–1 spectra also require a change in the inner disk radius during the *BeppoSAX* observation, which may be due to the nonphysical effects inherited in the model. In contrast, the CMCD model with the spheric corona gives the predictions of both the disk inclination angle and the absorption that are consistent with the direct measurements, and only slightly under-predicts the black hole mass of LMC X–3. The model explains the spectral state evolution of LMC X–1 within the *BeppoSAX* observation as a change in the accretion rate, which leads to an increase in both the inner disk temperature and the Comptonization opacity. On the other hand, the CMCD model with the slab-like corona is more problematic in the test and is thus not recommended.

Key words: black hole physics — stars : individual (LMC X–1, LMC X–3) — X-rays: stars

1 INTRODUCTION

Accreting black hole X-ray binaries (BHXBs) typically stay in one of the two distinct spectral states (Tanaka & Lewin 1995). In the so-called high/soft state, such a binary has a soft X-ray spectrum and a relatively high X-ray luminosity, which is believed to be dominated by the emission directly from the accretion disk around the black hole (BH). Under the standard geometrically thin and optically thick accretion disk approximation (see Pringle 1981 and references therein), the X-ray spectrum is an integration of the assumed blackbody-like emission over the disk with a temperature that decreases with increasing radius (Mitsuda et al. 1984) and is thus called the multi-color disk (MCD). In the opposite low/hard state, the spectrum is relatively flat and can often be approximated by a power law (PL), which may extend up to several hundred keV, whereas the luminosity is typically low. The flat spectral shape is usually attributed to the Comptonization of soft disk photons by hot electrons in a surrounding corona (e.g., Zdziarski 2000). Therefore the spectrum of a BHXB system can usually be well fitted by a two-component model with a blackbody-like (soft) component plus a PL-like (hard) component; a disk reflection component and a broad iron line component are sometimes also visible in the spectra of some systems (e.g., Cygnus X-1, Di Salvo et al. 2001; GX 339–4, Ueda, Ebisawa, & Done 1994).

Of course, there are various other effects that one needs to consider. For the soft component, because of the high temperature ($\sim$ 1 keV) in the inner region of the accretion disk, disk emission is expected to be slightly Comptonized by the free electrons in this region and the local emergent spectrum could be approximated as a diluted blackbody spectrum rather than a blackbody one. Furthermore, the emission from the inner accretion disk is subject to the strong gravitational field in the vicinity of the BH, and should also be modified by the extreme Doppler motion of the accretion disk. Detailed calculations suggest that the simple MCD model (diskbb in XSPEC) could still be used to describe the distorted disk emission, but needs to be corrected by several

⋆ E-mail:yaoys@astro.umass.edu

factors in order to infer the consistent physical quantities: a factor f_{color} accounting for the color temperature correction of the Comptonization in the inner disk region (e.g, Shimura & Takahara 1995; Merloni, Fabian, & Ross 2000); a factor η indicating the difference between the apparent and intrinsic radii of the peak temperature, and the integrated luminosity difference between the MCD model and a more realistic accretion disk with torque-free boundary condition (e.g., Kubota et al. 1998; Gierliński et al. 1999); factors f_{GR} and g_{GR} accounting for gravitational redshift and Doppler shift and the integrated disk flux change due to the general relativistic effects (e.g., Cunningham 1975; also see Zhang, Cui, & Chen 1997 for more discussions).

For the hard component, the phenomenological PL model is often used. However, the extrapolation of the PL model to the lower energy in the MCD+PL model neglects the seed photon curvature that should be reflected in the Comptonized spectrum (e.g., Shrader & Titarchuk 1998; Done, Życki, & Smith 2002). In a typical global fit of the MCD+PL model to a BHXB spectrum, this unphysical extrapolation usually leads to an artificial increase in the soft X-ray-absorbing column density estimates. As a result, the absorption-corrected source flux could be over-estimated. This problem is not very acute for an observation with poor counting statistics and/or for a low temperature accretion disk with the MCD emission peak located outside the observed energy range (e.g., accreting intermediate-mass BH candidates; Wang et al. 2004, Paper II). But for a stellar mass BH with an accretion disk temperature of ~ 1 keV, the problem is significant. In fact, it has been shown that the MCD+PL model fails to give an acceptable fit to X-ray spectra of LMC X–3, when the X-ray absorption is tightly constrained by an independent measurement from X-ray absorption edges in dispersed X-ray spectra (Page et al. 2003).

Instead of using the PL model, several groups have developed various Comptonization models by taking care of the radiative transfer process either numerically or analytically (e.g., *compbb*, Nishimura, Mitsuda, & Itoh 1986; *comptt*, Titarchuk 1994; Hua & Titarchuk 1995; *thcomp*, Życki, Done, & Smith 1999; *eqpair*, Coppi 1999 and references therein; *compps*, Poutanen & Svensson 1996; etc.). The seed photon spectrum is assumed to be a single-temperature blackbody in *compbb* or its Wien approximation in *comptt*, which clearly deviates from a multi-color black-body disk. This deviation could be very significant, especially for a disk with a high inner temperature, typical for a stellar mass BH; the black-body would peak well within an X-ray band. Whereas the *thcomp* is a thermal Comptonization model, the *eqpair* model is a hybrid model of thermal and non-thermal Comptonization (see also Gierliński et al. 1999); both models can adopt a proper disk spectrum, but the latter is more advanced which takes care of nearly all the important physical processes in a disk-corona system including Compton scattering, pair production and annihilation, bremsstrahlung, and synchrotron radiation, etc. (Coppi 1992). All these four models can only produce a direction-averaged spectrum. Like *eqpair* model, the *compps* model also contains most physical processes in the disk-corona system and allows the use of a MCD spectrum, but it can treat geometry more accurately and generate an angular dependent spectrum in a spherical or a slab-like corona system.

It is worth noting that in the disk-corona scenario, the Comptonization generates the PL-like component at the expense of the MCD flux, therefore the MCD and the PL-like components are physically related. Some Comptonization models mentioned above (e.g., *eqpair* and *compps*) have taken care of this relationship whereas some have not (e.g., *thcomp*). One then should be cautious of interpreting the physical meaning of the MCD parameters when applying the Comptonization models. The MCD model here describes only those un-Comptonized (un-scattered or escaped) disk photons rather than the actually original disk emission. In particular, this relationship does not exist in MCD+PL model, therefore the original disk flux could be under-estimated from the fitted MCD parameters, so are other related inferred parameters such as inner disk radius. The under-estimate, for example, may be responsible for the *apparent* change in the inner disk radius with the transition from one state to another, as has been claimed for several sources such as XTE J1550-564, GRO J1655-40 (Sobczak et al. 1999a,b), and XTE J2012+381 (Campana et al. 2002).

All the models mentioned above have been widely used to model the spectra of Galactic BHXBs, neutron star X-ray binaries, as well as the extragalactic sources including ultraluminous X-ray sources (ULXs) and AGNs. However, except for the works by Gierliński et al. (1999, 2001), there has been little rigorous test of the models against direct measurements (e.g., neutral absorption column density, BH mass, system inclination, etc.), which are available for several well-known systems such as GRO J1655–40, LMC X–1, and LMC X–3.

In Yao et al. (2005; Paper I), we have presented a Monte-Carlo method in simulating Comptonized multi-color disk (CMCD) spectra. The simulations used the MCD as the source of seed photons and self-consistently accounted for the radiation transfer in the Comptonization in a spherical or slab-like thermal plasma. We have applied this CMCD model, implemented as a table model in XSPEC, to a stellar mass BH candidate XTE J2012+381 in our Galaxy. This application shows that the inner disk radius is *not* required to change when the source transits from the soft state to the hard state, in contrast to the conclusion reached from the fits with the MCD+PL model (Campana et al. 2002). For a spherical corona, the toy model contains the following parameters: the inner disk temperature (T_{in}), the system inclination angle (θ), the effective thermal electron temperature (T_c), optical depth (τ), and radius (R_c) of the corona as well as the normalization defined as

$$K_{CMCD} = \left(\frac{R_{in}/\mathrm{km}}{D/10\mathrm{kpc}} \right)^2 , \quad (1)$$

where D is the source distance and R_{in} is the apparent inner disk radius. For a slab-like corona, another extreme of the geometry, we assume that the corona covers the whole accretion disk. We find that the final emerged spectra are insensitive to the different vertical scales, so R_c does not appear as a parameter in this geometry. Note that K_{CMCD} differs from the normalization for the MCD model,

$$K_{MCD} = \left(\frac{R_{in}/\mathrm{km}}{D/10\mathrm{kpc}}\right)^2 \cos(\theta). \quad (2)$$

More detailed discussion on the CMCD model can be found in Paper II, in which we have applied the same model for a spherical geometry to six ULXs observed with *XMM-Newton*. The fitted T_{in} ($\sim$ 0.05–0.3 keV) of these sources are distinctly different from the values ($\sim$ 1 keV) obtained for known stellar-mass BHs, as presented in this paper and in Paper I. Indeed, the inferred BH masses (M_{BH}) of the ULXs are $\sim 10^3 M_\odot$, consistent with the intermediate-mass BH interpretation of these sources. We have also shown that the MCD+PL model gives an equivalent spectral description of the ULXs, although the CMCD model provides unique constrains on the corona properties and on the disk inclination angles, as well as on the BH masses. Because of the lower disk temperatures, compared to those of the stellar mass BH systems, the nonphysical effects of the MCD+PL model are typically not significant in the observable photon energy range of the intermediate-mass BH candidates.

In the present work, we conduct a critical test of the CMCD and MCD+PL models by comparing parameters (M_{BH}, θ, and the equivalent neutral hydrogen absorption N_H) inferred from the X-ray spectra of LMC X–1 and X–3 with the more direct measurements based on optical and dispersed X-ray spectra; we also compare the results from the different corona geometrical configurations of the CMCD model. We first briefly describe these measurements and the X-ray observations in §2, and then present the spectral fitting results in §3. We describe the specific comparisons in §4 and present the discussion and our conclusions in §5.

2 DESCRIPTION OF THE SOURCES AND OBSERVATIONS

We select LMC X–1 and X–3 for this study chiefly because of their location in our nearest neighboring galaxy, the Large Magellanic Cloud (LMC; $D = 50$ kpc is adopted throughout the work). Both the well-determined distance and the relatively low foreground soft X-ray absorption are essential to our test. These two sources are also among the three well-known persistent BHXBs and are usually found in the high/soft state. The low/hard state was occasionally reported for LMC X–3 (Boyd & Smale 2000; Homan et al. 2000), but never for LMC X–1. The remaining known persistent BHXB, Cygnus X–1, is in our Galaxy and stays mostly in the low/hard state (e.g., Pottschmidt et al. 2003). The X-ray spectra of this source also show a strong disk reflection component (Gilfanov et al. 1999; Frontera et al. 2001) — a complication that is not included in the CMCD models. Table 1 summarizes the key parameters of LMC X–1 and X–3, which are used for the comparison with our spectrally inferred values (§4).

Both LMC X–1 and X–3 were observed with *Chandra* (e.g., Cui et al. 2002) and *XMM-Newton* (e.g., Page et al. 2003). The dispersed X-ray spectra of LMC X–3 have been used to measure the X-ray absorption edges (mainly for Oxygen), which tightly constrains the the absorbing matter column density N_H along the line of sight (Page et al. 2003). The absorption towards LMC X–1 is, however, substantially higher. As a result, the photon flux at the Oxygen edge is too low to allow for a useful constraint on N_H based on the existing data.

We here utilize the data from the *BeppoSAX* observations, which were carried out on 1997 October 5 for LMC X–1 and October 11 for X–3 (Treves et al. 2000). The data do not have pile-up problems, which could be present for X-ray CCD imaging observations of bright sources. Four types of narrow-field instruments (NFIs) were on board: Low Energy Concentrator System (LECS), Medium Energy Concentrator Systems (MECS), High Pressure Gas Scintillation Proportional counter (HPGSPC), and Phoswich Detector System (PDS) (Boella et al. 1997). The exposure for LMC X–1 and X–3 were about 15 ks each for the LECS and about 40 ks each for the MECS. These two instruments were sensitive to X-rays in the energy ranges of 0.1–10 and 1.3–10 keV respectively. Data from the HPGSPC and the PDS, which were sensitive to photons in 4–120 keV and 15–300 keV ranges respectively, were not included because of poor counting statistics, and also because of possible source contamination from PSR 0540–69 (which is $25'$ away from LMC X–1) (Seward et al. 1984; Haardt et al. 2001). We extracted the spectra from a radius of $8'$ and $8.4'$ around each source from the LECS and the MECS observations and used the energy ranges of 0.2–4 keV and 1.8–10 keV for these two instruments in this study. The background contributions to the spectra are small and are estimated from a blank field. The spectra from the LECS, the MECS2, and the MECS3 were jointly fitted for each source, using the software package XSPEC*11.2.0bs*.

3 RESULTS

We summarize the spectral fitting results and the inferred source fluxes in Table 2. The quoted uncertainty ranges of the parameters are all at 90% confidence level. Fig. 1 shows the spectral fits with the CMCD models. The systematic deviation of the data from the model at low energies ($\lesssim$ 1 keV) might be due to poor calibration of the instrument spectral response (Martin et al. 1996). Fig. 2 illustrates the effects of the Comptonization in the spherical corona systems.

Both CMCD and MCD+PL models give acceptable fits. The model parameters are all well constrained except for the CMCD parameter θ, for which only the upper or lower limit is constrained. The MCD+PL model parameters we obtained here are consistent with those reported by Haardt et al. (2001). The fitted N_H values from MCD+PL are systematically higher than those from CMCDs. The same is true for the inferred absorption-corrected fluxes, especially for LMC X–1 which is a factor of $\sim$ 4 higher from MCD+PL than from CMCD (Table 2).

For LMC X–3, T_{in} from MCD+PL is slightly higher than those from CMCDs, whereas the value of $K_{MCD}/\cos(\theta)$ is consistent with those of K_{CMCD}. The best fit parameters in the two different geometric CMCDs are nearly identical. The small value of τ_c indicates that only a small portion of disk photons have been up-scattered to high energies.

For LMC X–1, except for a consistent N_H value, the fitted parameters are significantly different between the two different geometric CMCDs (Table 2). We will see in §4, the results from the slab-like configuration are inconsistent with the independent measurements. T_{in} values from the

Table 1. Comparison of parameter measurements.

	θ (°)	M_{BH} ($M_\odot$)	N_H ($10^{20}cm^{-2}$)	T_{in} (keV)	References
		LMC X–1			
Indep. est.	$24 \leqslant \theta \leqslant 64$	$4 \leqslant M \leqslant 12.5$	–	–	1, 2
CMCD: sphere	$\lesssim 43$	4.0(3.8–4.5)	54(52–56)	0.93(0.91–0.94)	
CMCD: slab	$\gtrsim 64$	15.2(10.4–19.9)	53(51–54)	0.80(0.79–0.81)	
MCD+PL	N/A	3.0(2.9–3.1)	84(79–89)	0.93(0.92–0.95)	
		LMC X–3			
Indep. est.	$\theta \leqslant 70$	$M > 5.8 \pm 0.8$	3.8(3.1–4.6)	–	3,4,5,6
CMCD: sphere	$\lesssim 69$	4.19(4.17–4.21)	4.5(4.2–4.7)	0.98(0.97–0.99)	
CMCD: slab	$\lesssim 61$	3.73(3.71–3.76)	4.4(4.2–4.6)	0.96(0.95–0.97)	
MCD+PL	N/A	4.2(4.1–4.3)	7.0(6.0–8.0)	1.02(1.01–1.03)	

The BH mass M_{BH} is estimated by assuming zero spin of the BH. See text for details. References: [1] Hutchings et al. (1983); [2] Gierliński et al. (2001); [3] Cowley et al. (1983); [4] Paczynski (1983); [5] Soria et al. (2001); [6] Page et al. (2003).

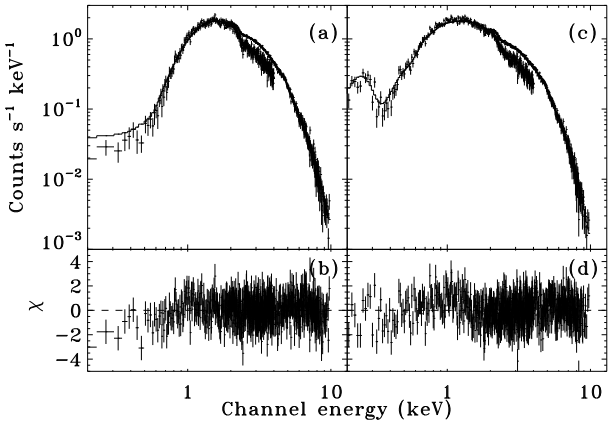

Figure 1. Model fits to the *BeppoSAX* spectra of LMC X–1 (*panel a*) and LMC X–3 (*panel c*), and the corresponding residuals in term of sigmas (*panels b* and *d*). The *solid line* in *panels a* and *c* show the fit of CMCD model. The fit goodnesses from the different geometrical models (a sphere vs. a slab) are nearly the same.

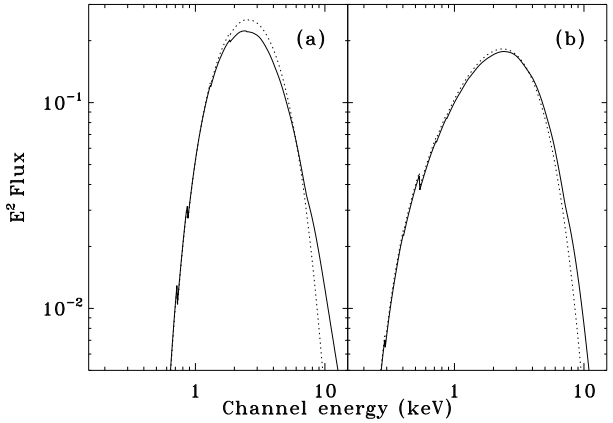

Figure 2. The effects of the Comptonization in LMC X–1 (*a*) and in LMC X–3 (*b*). *Solid line*: spherical CMCD model with the best fit parameters; *dotted line*: CMCD model with the same parameters but τ=0, which is equivalent to the MCD model.

Table 2. Spectral fit results

parameters	LMC X–1	LMC X–3
	CMCD: sphere	
N_H (10^{21} cm^2)	5.4(5.2–5.6)	0.45(0.42–0.47)
T_{in} (keV)	0.93(0.91–0.94)	0.98(0.97–0.99)
T_c (keV)	19(15–23)	20(19–23)
R_c (R_g)	11(9–19)	10.0(9.6–16.6)
τ	1.0(0.8–1.3)	0.10(0.09–0.13)
θ (deg)	28(**–43)	59(**–69)
$K_{\rm CMCD}$	57(51–73)	44.0(43.5–44.3)
χ^2/dof	641/627	760/649
$f_{0.2-10}$	8.6	5.7
	CMCD: slab	
N_H (10^{21} cm^2)	5.3(5.1–5.4)	0.44(0.42–0.46)
T_{in} (keV)	0.80(0.79–0.81)	0.96(0.95–0.97)
T_c (keV)	10.0(9.0–10.6)	22(19–24)
τ	0.45(0.41–0.49)	0.09(0.08–0.12)
θ (deg)	75(64–**)	50(**–61)
$K_{\rm CMCD}$	489(230–840)	42.7(42.1– 43.3)
χ^2/dof	638/628	759/650
$f_{0.2-10}$	8.5	5.7
	MCD+PL	
N_H (10^{21} cm^2)	8.4(7.9–8.9)	0.7(0.6–0.8)
T_{in} (keV)	0.93(0.92–0.95)	1.02(1.01–1.03)
$K_{\rm MCD}$	28(26–30)	23(22–24)
Γ	3.5(3.4–3.6)	2.6(2.5–2.8)
K_{PL} (10^{-1})	2.3(1.9–2.7)	0.19(0.14–0.23)
χ^2/dof	624/629	747/651
$f_{0.2-10}$	31	6.4

The uncertainty ranges are given in parenthesis at the 90% confidence level; asterisks indicate that the limit is not constrained. $R_g = GM/c^2$. The $f_{0.2-10}$ is the absorption-corrected flux in the energy range 0.2–10 keV and in unit of 10^{-10} erg cm^{-2} s^{-1}.

spherical CMCD and the MCD+PL are consistent with each other, but $K_{MCD}/\cos(\theta)$ value, assuming the best-fit CMCD θ, is ~ 1.5 smaller than K_{CMCD}.

Because a significant change in the spectral shape occurred during the observation of LMC X–1, we have further split the exposure into two parts, the first 30 ks and the remaining time, in the same way as in Haardt et al. (2001). To tighten the constraints on spectral parameters, we jointly fit N_H and θ, which should be the same in the two parts of the observation (Table 3). From the early part to the later part, according to the spherical CMCD model, T_{in} increased by $\sim 7\%$ and the corona became a factor of ~ 2 larger and opaque with τ increased by a factor of ~ 4.

Table 3. Spectral variation of LMC X–1

parameters	part 1	part 2
	CMCD: sphere	
N_H (10^{21} cm^2)	5.3(5.2–5.5)	= part 1
T_{in} (keV)	0.91(0.90–0.92)	0.96(0.93–0.99)
T_c (keV)	13(9–18)	10(8–12)
R_c (R_g)	10(9–16)	25(18–33)
τ	0.55(0.5–0.7)	2.0(1.8–2.4)
θ (deg)	23(**–45)	= part 1
K_{CMCD}	61(55–72)	57(46–77)
χ^2/dof	1211/1192	
$f_{0.2-10}$	8.8	8.3
	CMCD: slab	
N_H (10^{21} cm^2)	5.3(5.2–5.4)	= part 1
T_{in} (keV)	0.81(0.80–0.82)	0.74(0.73–0.76)
T_c (keV)	20(19–23)	5(**–7)
τ	0.11(0.10–0.14)	1.9(1.7–2.1)
θ (deg)	75(64–**)	= part 1
K_{CMCD}	348(224–495)	1223(730–1855)
χ^2/dof	1209/1194	
$f_{0.2-10}$	8.8	8.1
	MCD+PL	
N_H (10^{21} cm^2)	8.5(8.0–9.0)	= part 1
T_{in} (keV)	0.90(0.89–0.91)	1.00(0.98–1.03)
K_{MCD}	52(49–55)	23(21–26)
Γ	3.6(3.5–3.8)	3.4(3.3–3.6)
K_{PL} (10^{-1})	3.0(2.4–3.7)	3.4(2.8–3.9)
χ^2/dof	1180/1195	
$f_{0.2-10}$	48	42

Please refer to Table 2.

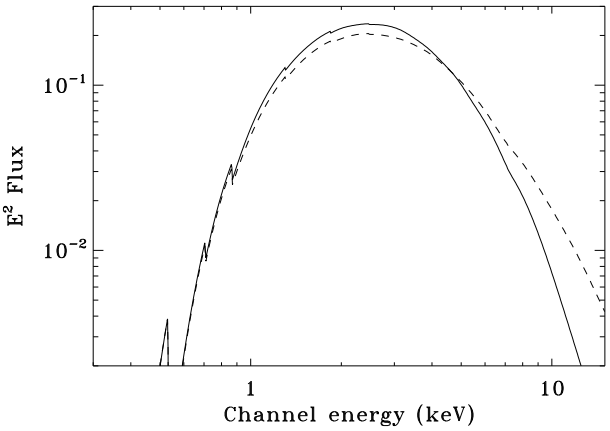

Figure 3. The spectral variation of LMC X–1 from the first 30 ks (part 1, *solid line*) to the remaining time (part 2, *dashed line*). The models are plotted with the best fitting parameters (Table 3).

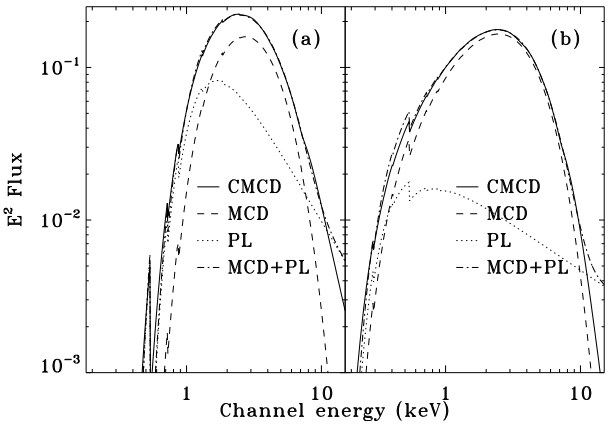

Figure 4. The comparison of the spherical CMCD model and MCD+PL model with the best fit parameters (Table 2) for (*a*) LMC X–1 and (*b*) LMC X–3.

The source flux in the 0.2-10 keV band decreased slightly, although the normalization remained essentially the same. Because $T_{in} \propto (\dot{M}/M_{BH})^{1/4}$, where M_{BH} and $\dot{M}$ are the BH mass and the accretion mass rate, a rising T_{in} during the observation of LMC X–1 was then caused by an increasing accretion rate. Apparently, this change led to the thickening of the corona. The slight decline of the flux is likely due to a combination of the energy loss to the corona and to the scattering of photons to energies greater than $\gtrsim$ 10 keV. Fig. 3 demonstrates the differences of the Comptonization effects in the two parts of the observation. However, it is hard to physically understand the fitted parameters of the slab-like CMCD: From early part to the later part, T_{in} and T_c need to decrease by $\sim$ 16% and a factor of 4, respectively, but in the mean time both τ and K_{CMCD} (hence R_{in}) have to increase dramatically. We believe that the slab-like CMCD model is not suitable for describing such a spectral state of a BHXB system when the hard component contributes significantly to the total flux.

Now let us check the results from the MCD+PL model, which are fairly consistent with those of Haardt et al. (2001). The MCD normalizations are significantly different between the early and later parts of the observation (Table 3), confirming the analysis by Haardt et al. (2001), which is based on the same data and same model. They concluded that as T_{in} increased (by $\simeq$ 9%), R_{in} decreased ($\simeq$ 38%) from the early to later parts of the observation. But, as was discussed in §1, this apparent change in R_{in} is most likely due to the lack of the accounting for the radiative transfer between the two components of the MCD +PL model and is therefore not physical.

Furthermore, Fig. 4 shows clearly that for both sources, the PL component surpasses the MCD component in contributing to the spectra at low energies ($\lesssim$ 1 keV for LMC X–1 and $\lesssim$ 0.4 keV for LMC X–3). This nonphysical straight extension of the PL component to the low energy parts of the spectra is the main cause for the required high values of N_H in the MCD+PL fits, compared to those in the CMCD fits (Tables 2 and 3).

4 COMPARISONS WITH INDEPENDENT MEASUREMENTS

In addition to the above self-consistency check of the X-ray spectral models, we compare the inferred parameter values of the BHXBs with the independent measurements to further the test. The key results of this comparison are included in Table 1 and are discussed in the following:

• **X-ray Absorption** N_H may be obtained more directly and accurately via the spectroscopy of neutral absorption edges of Oxygen and Neon (e.g., Schulz et al. 2002; Page et al. 2003). This method is nearly independent of the overall continuous spectral shape and any other source prop-

erties. Using the dispersed spectrum of an *XMM-Newton* observation, Page et al. (2003) inferred $N_H = 0.38^{+0.08}_{-0.07} \times 10^{21}$ cm^{-2} for LMC X–3, assuming the interstellar medium abundance of Wilms et al. (2000). We have also adopted this assumption by using the absorption model *TBabs* in XSPEC. The N_H values from the CMCD models and from the X-ray absorption edge measurement agree with each other within the quoted error bars, whereas the value from the MCD+PL model is significantly higher (Table 1).

• **Disk Inclination Angle** The upper limits on θ from the spherical CMCD model are consistent with the values obtained from the optical observations (Table 1). There is a simple reason why θ can be constrained in the spherical CMCD model: the Comptonized flux is nearly isotropic and barely affected by the disk inclination, whereas the observed strength of the soft disk component is proportional to $\cos(\theta)$. This mostly geometric effect is strong when θ is large; e.g., no radiation come directly from an edge-on disk. Therefore, the upper limit can be constrained reasonably well, which is especially important for estimating the BH mass (cf. Eqs. 1 and 2). In the slab-like CMCD model, since both of the observed soft and hard components strongly depend upon the system inclination angle (e.g., Sunyaev & Titarchuk 1985; see also the Fig. 2 in Paper I), θ in principle can be well constrained in this model. For LMC X–3, the PL-like component only contributes a small portion of the total flux, and the constraint of θ mainly from the soft component, as in a spherical CMCD model. For LMC X–1, the PL-like component contributes significantly to the total flux. The slab-like corona configuration becomes problematic, giving the inconsistent θ constraints.

• **Black Hole Mass** The mass of each putative BH may be estimated as $M = c^2 f R_{in}/G\alpha$, where $\alpha = 6$ or 1 for a non-spin or extreme spin BH), fR_{in} is the inner disk radius, assumed to be the same as the radius of the last marginally stable orbit around the BH, and the factor f [depending on the system inclination, 0.94 for LMC X–1 and 1.12 for LMC X–3; we adopt a new value of $\eta = 0.41$ (see §1) derived from Kubota et al. (1998), compared to the old values used $\eta = 0.7$ used in Zhang et al. (1997) and in Paper II] includes various corrections related to the spectral hardening, special and general relativity effects (e.g., Cunningham 1975; Zhang, Cui, & Chen 1997; Gierliński et al. 1999, 2001). Assuming no spin for the BHs, from the spherical CMCD results, we estimate the BH masses as 4.0(3.8–4.5), 4.19(4.17–4.21) $M_\odot$ for LMC X–1 and LMC X–3, respectively. For LMC X–1, the value is consistent with the result from the optical study, whereas for LMC X–3, the derived M_{BH} is slightly smaller (Table 1) which may suggest that the LMC X–3 is a mild spin system.

5 SUMMARY

In this work, we have applied the MCD+PL model as well as our recently constructed CMCD model to BHXB systems LMC X–1 and LMC X–3, confronting the fitted parameters with directly measured values. We have also tested two different corona geometric configurations. The spherical configuration passes almost all the tests: the effective hydrogen column densities, disk inclinations, and the BH masses of the LMC X–1 and LMC X–3. This consistency suggests that the CMCD model with a spherical corona provides a reasonably good spectral characterization of BHXBs. The model offers useful insights into physical properties of the Comptonization coronae and their relationship to the accretion process. In contrast, the slab-like CMCD model is problematic in describing the spectrum of LMC X–1, in which the PL-like component contributes significantly. Similarly, the MCD+PL model, though generally providing a good fit to the spectra of BHXBs, could give misleading parameter values. Although the tests conducted in this work are still very limited, they have demonstrated the potential in discriminating among various models.

ACKNOWLEDGMENTS

We thank the anonymous referee for his/her insightful comments on our manuscript which helps us to improve the paper greatly. Y. Yao is also grateful to Xiaoling Zhang and Yuxin Feng for their useful discussions.

REFERENCES

Boella, G., et al. 1997, A&AS, 122, 327
Boyd, P. T. & Smale, A. P. 2000, IAU Circ., 7424, 3
Campana, S., et al. 2002, A&A 384, 163
Coppi, P. S., 1992, MNRAS, 258, 657
Coppi P. S., 1999, in Poutanen J., Svensson R., eds, ASP Conf. Ser. Vol. 161, High Energy Processes in Accreting Black Holes. Astron. Soc. Pas., San Francisco, p. 375
Cowley, A. P., et al. 1983, ApJ, 272, 118
Cui, W., et al. 2002, ApJ, 576, 357
Cunningham C. T., 1975, ApJ, 309, 788
Done, C., Życki, P. T., & Smith, D. A. 2002, MNRAS, 331, 453
Frontera, F., et al. 2001, ApJ, 546, 1027
Gierliński, M., et al. 1999, MNRAS, 309, 496
Gierliński, M., Maciołek-Niedźwiecki, A., & Ebisawa, K. 2001, MNRAS, 325, 1253
Gilfanov, M., Churazov, E., & Revnivtsev, M. 1999, A&A, 352, 182
Haardt, F., et al. 2001, ApJ, 133, 187
Homan, J., et al. 2000, IAU Circ.,7425, 2
Hua, X.-M. & Titarchuk, L. 1995, 449, 188
Hutchings, J. B., Crampton, D., & Cowley, A. P. 1983, ApJ, 275, L43
Kubota, A., et al. 1998, PASJ, 50, 667
Martin, D., et al. 1996, In EUV, X-Ray, and Gamma-Ray Instrumentation for Astronomy VII, O. Siegmund, M. Gummin eds., SPIE Proceedings Vol. 2808.
Merloni, A., Fabian A. C., & Ross, R. R. 2000, MNRAS, 313, 913
Mitsuda, K., et al. 1984, PASJ, 36, 741
Nishimura, J., Mitsuda, K., & Itoh, M. 1986, PASJ, 38, 819
Paczynski, B. 1983, ApJ, 273, L81
Page, M. J., et al. 2003, MNRAS, 345, 639
Pottschmidt, K., et al. 2003, A&A, 407 1039
Poutanen, J., & Svensson, R. 1996, ApJ, 470, 249
Pringle, J. E. 1981, ARA&A, 19, 137
Di Salvo, T., Done, C, Zycki, P. T., Burderi, L., & Robba, N. R. 2001, ApJ, 547, 1024

Schulz, N. S., et al. 2002, ApJ, 565, 1141
Seward, F. D., Harnden, F. R., & Helfand, D. J. 1984, ApJ, 287, L19
Shimura, T., & Takahara, F. 1995, ApJ, 445, 780
Shrader, C., & Titarchuk, L., 1998, ApJ, 499, L31
Sobczak, G. J., et al. 1999a, ApJ, 517, L121
Sobczak, G. J., et al. 1999b, ApJ, 520, 776
Soria, R., et al. 2001, A&A, L273
Sunyaev, N. I., & Titarchuk, L. 1985, A&A, 143, 374
Tanaka, Y. & Lewin, W. H. G. 1995, in X ray Binaries, eds. W.H.G. Lewin, J. van Paradijs and E.P.J. van den Heuvel, (Cambridge U. Press, Cambridge) 126 174
Titarchuk, L. 1994, ApJ, 434, 313
Treves, A., et al. 2000, Adv. Space Res., 25, 437
Ueda, Y., Ebisawa, K., & Done, C. 1994, PASJ, 46, 107
Wang, Q. D., Yao, Y., Fukui W., Zhang, S. N., & Williams, R. 2004, ApJ, 609, 113
Wilms, J., Allen, A., & McCray, R. 2000, ApJ, 542, 914
Yao, Y., Zhang, S. N., Zhang, X., Feng, Y., & Robinson, C. R. 2005, ApJ, 619, 446
Zdziarski, A. A. 2000, IAUS, 195, 153
Zhang, S. N., Cui, W., & Chen, W. 1997, ApJ, 482, 155
Życki, P. T., Done, C., & Smith, D. A. 1999, MNRAS, 309, 561